ESRF	**Experiment title:** In situ calorimetry and threshold phenomena of laser-excited metal nanoparticles	**Experiment number:** SC5032
Beamline: ID19	**Date of experiment:** from: 10-03-2021 16-03-2021	**Date of report:** 5/9/2021
Shifts: 18	**Local contact(s):** M. Levantino	*Received at ESRF:*

Names and affiliations of applicants (* indicates experimentalists):

Dr. A. Plech*, (KIT Karlsruhe), single local user

A. Ziefuss*, Dr. S. Reichenberger* (U. Duisburg-Essen), remote users

Report summary:

The pulsed laser irradiation and excitation of metal nanoparticles is used in different applications, such as nanoparticle size tailoring [1] (as fragmentation or melt-induced reshaping) or photothermal applications [2]. While solid knowledge exists about the excitation pathway (electron excitation, electron-electron scattering, electron-phonon coupling), processes like the energy dissipation (particles cooling with the environment), the initiated structural transitions (such as melting), and the absolute excitation density of otherwise well described optical properties of the nanoparticles in suspension still poses a lot of open questions and mysteries.

An example of such an unexpected behavior was the observation that the excitation of gold nanoparticles with a pulsed laser wavelength around the plasmon resonance (SPR) of 532 nm surprisingly showing a significantly lower particle heating and hence a higher reaction (fragmentation/size reduction) threshold than theoretically expected [3, 4, 5] from Mie theory.

Consequently, the present experiment was intended to secure and quantify the previous experimental observation and expand towards a general mechanism. We excited spherical gold nanoparticles of a large range of sizes from 13 to 167 nm and different surface functionalization and crystallinity (from different synthesis pathways) [1] with 1 ps laser pulses at two laser wavelengths (resonant excitation at 532 nm vs interband excitation at 400 nm). The interband absorption (IB) at 400 nm promotes electrons from the 5d to the 6s band for wavelengths shorter than approx. 500 nm (Fermi level) (see fig. 1). Intraband absorption, on the other hand, leads to the prominent SPR resonance that is size-selective and ranges from 515 to 550 nm for particle diameters of 10 to 80 nm [11]. To investigate these different excitation channels the lattice expansion at 60 ps delay was compared for 400 nm and 532 nm.

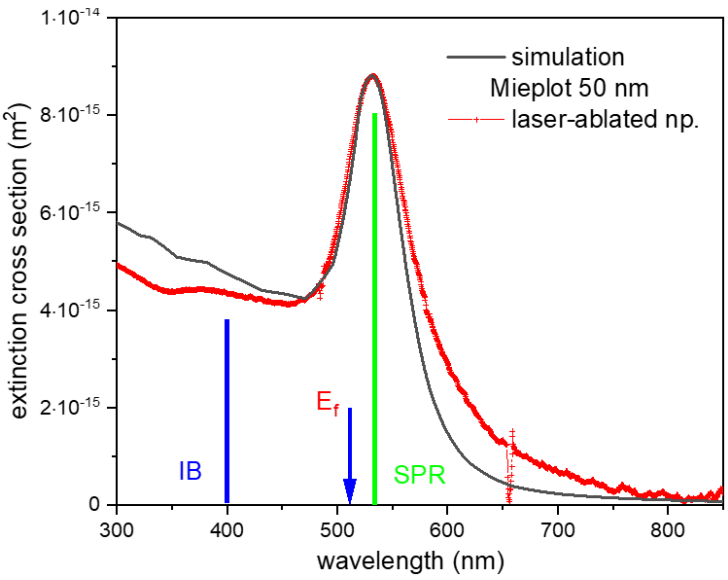

Fig. 1: Optical extinction spectrum of laser-ablated gold particles in water (red symbols) compared to a simulation by Mie theory (black line, Mieplot, P. Laven). Interband excitation is possible for wavelengths below the Fermi level E_f with the intraband SPR resonance located close to 532 nm. The blue and green lines mark the laser excitation wavelength, respectively.

Experimental setup:
The experiment used the typical setup at ID09, where a quasimonochromatic X-ray beam with single-pulse trains at 1 kHz is focused on a liquid jet containing the gold particles. The jet was driven by a syringe pump and formed freely in the air with a diameter of 0.26 mm after exiting a round capillary. The aqueous suspension was excited by time-delayed laser pulses coming from the frequency-doubled regenerative amplifier (at 400 nm) or after parametric wave mixing in the TOPAS device to produce 532 nm. The laser beam was focused onto the jet with reduced pupils to increase the size of the Airy disk. Hence, a smooth intensity profile across the beam was achieved. Pulse energy and thus laser fluence was controlled by a stepper-actuated rotating waveplate in front of a linear polarizer. Much care was taken to quantify the laser cross section, stability, and definition of fluency.

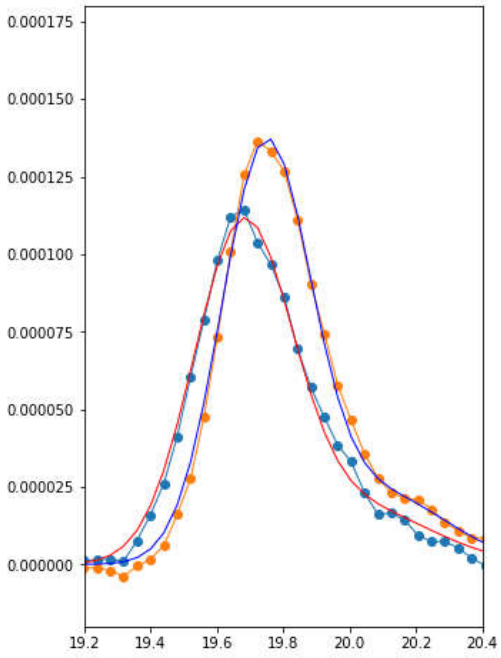

Fig. 2a: *Angular profile (detector angle) of the gold (111) reflection gefore laser excitation (yellow bullets) and 60 ps after laser excitation (blue bullets) together with asymmetric Gaussian fits to the profile.*

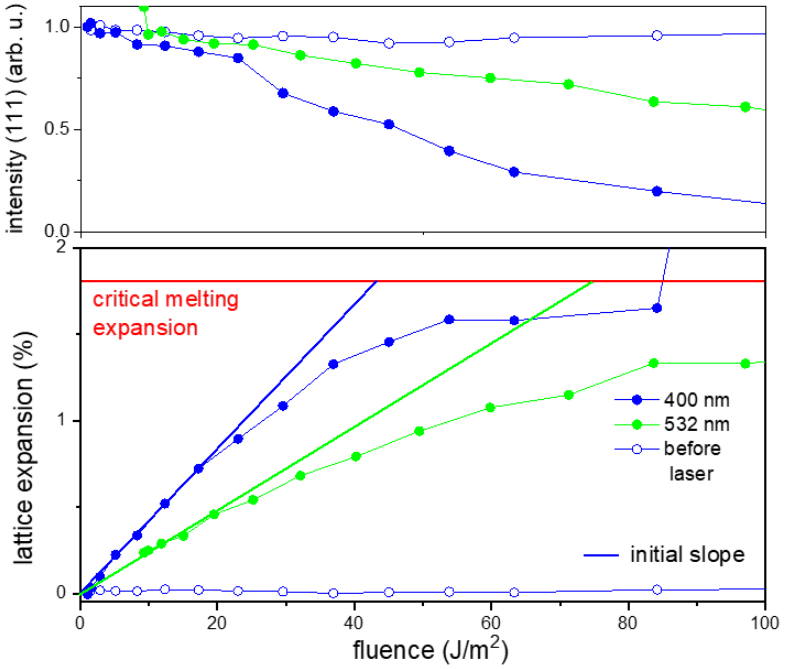

Fig. 2b: *Lattice expansion (lower graph) and intensity of (111) powder ring as function of laser fluence. At 1.78 % the lattice expansion reaches that of bulk gold at the melting point.*

This experiment used the new EBS beam for the first time for these nanoparticle suspensions. We could both profit from the decreased x-ray focus size (due to reduced source size and new toroidal mirror) and the cleaner spectral shape of the undulator emission at 15 keV, at closed gap operation of the U17 undulator. The smaller beam size was very helpful for only probing the center of the laser spot distribution on the sample. This helped keep the fluence variation at a minimum.
The narrow spectral profile allowed for a higher angular resolution of the powder rings from the gold particles. For the smaller particles, the Scherrer width was dominated by crystal size effects. For best fit we included a slightly asymmetric x-ray spectrum with a 1.7 % width to fully model the (111) and (200) reflections. These reflections were used to derive lattice expansion and melting. Selected baseline-corrected scattering profiles are shown in fig. 2a.

Results:
An analysis of the lattice expansion as a function of laser fluence shows an initially linear slope as expected for laser absorption and transformation into heat for a quantitative transformation of energy for both wavelengths [6]. However, the data in fig. 2b already shows drastically that the slope for 532 nm is lower than for 400 nm, although the extinction in fig. 1 (as well as absorption, not shown) suggests otherwise. The slope for 532 is much smaller than for 400 nm, while the absorption cross cross section would imply a twice higher energy uptake at 532 nm. Above a lattice expansion of 1 -1.2 %, the particles react with partial melting, when approaching the melting temperature. While the predicted lattice expansion for 400 nm coincides well with the measurements of the set of samples in fig. 3, the measured lattice expansion for 532 nm is strongly reduced and in direct comparison to 400 nm much lower. This proves the earlier observed discrepancy in excitation density. The discrepancy is apparently independent

of particle size as well as nanoparticle crystal structure and functionalization (ligands from chemical synthesis(or crystallinity [2] – high for seeded growth, low for citrate reduction of gold salt [7]).

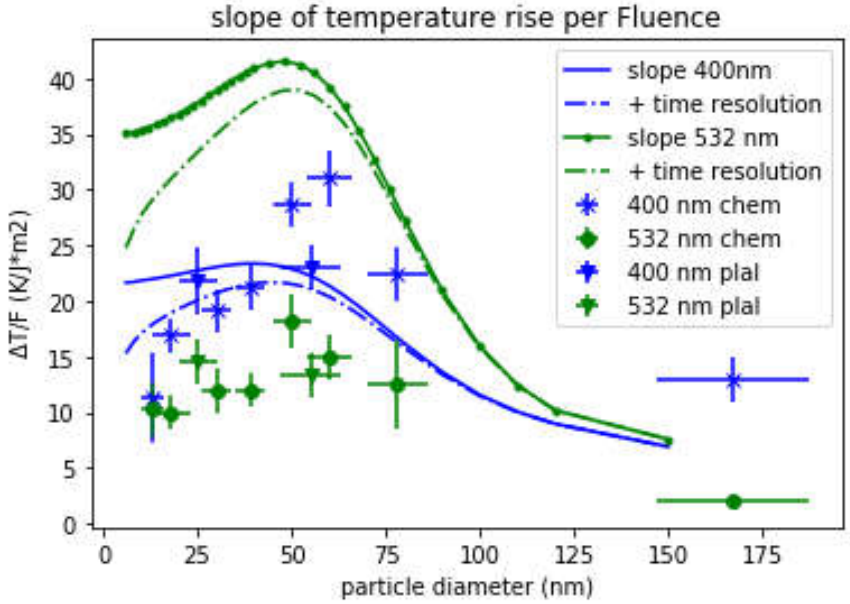

Fig. 3: Slope of temperature rise versus laser fluence for the full set of nanoparticles for different sizes and synthesis (chemical or laser-ablated). The lines are calculations of the expected slope if the apparent absorption translates fully into energy uptake and lattice heating. For the smallest particles, the limited time resolution at ID09 (60-80ps) leads to a reduction in sensitivity due to fast cooling to the medium, included in the calculation by dashed lines.

Conclusions:

The obtained data shows convincingly that there is a discrepancy in excitation density of gold nanoparticles excited either at the interband transition or the plasmon peak. This discrepancy can be explained by transient bleaching at the SPR. After excitation of the SPR, the electron temperature of the conduction electron increases strongly, leading to a plasmon suppression [8-10]. As the electronic heating by absorbed laser photons takes place within 10's of femtoseconds the related plasmon bleaching causes a significantly lower absorption efficiency of the laser pulse than theoretically expected. The IB on the other hand represents a direct excitation of different electronic energy states and hence is barely affected by transient bleaching effects [3, 8] such that a better agreement between experimental and theoretical results is to be expected. The electron-phonon coupling is slow (5 ps), which means that any few-ps pulse for excitation will sense this effect and the ability to absorb light is reduced at 532 nm.

References:

[1] S. Reich, A. Letzel, A. Menzel, N. Kretzschmar, B. Gökce, S. Barcikowski, A. Plech, *Nanoscale* 11 (2019) 6962 - 6969.
[2] L. R. Hirsch, R. J. Stafford, J. A. Bankson, S. R. Sershen, B. Rivera, R. E. Price, J. D. Hazle, H. J. Halas, J. L. West, *Proc Natl. Soc. Am.* 100 (2003) 13549.
[2] S. Ibrahimkutty, P. Wagener, A. Menzel, A. Plech, S. Barcikowski, *APL* 101 (2012) 103104.
[3] M. Magnozzi, R. Proietti Zaccaria, D. Catone, P. O'Keeffe, A. Paladini, F. Toschi, A. Alabastri, M. Canepa, F. Bisio, *J. Phys. Chem. C* 123 (2019) 16943−16950
[4] A. Ziefuß, S. Reich, S. Reichenberger, M. Levantino, A. Plech, *PCCP* 22 (2020) 4993-5001.
[5] A. Plech, S. Ibrahimkutty, S. Reich, G. Newby, *Nanoscale,* 9 (2017) 17284-17292.
[6] A. Plech, V. Kotaidis, S. Grésillon, C. Dahmen and G. von Plessen, *Phys. Rev. B* 70 (2004) 195423.
[7] J. Kimling, M. Maier, V. Kotaidis, B. Okenve, H. Ballot, A. Plech, *J. Phys. Chem. B* 110 (2006) 15700.
[8] M. Strasser, K. Setoura, U. Langbein, S. Hashimoto, *J. Phys. Chem. C 118* (2014), 25748.
[9] C Sönnichsen, T Franzl, T Wilk, G von Plessen, J Feldmann, *New J. Physics* 4 (2002) 93.1–93.8
[10] G. V. Hartland, *Phys.Chem.Chem.Phys.* 6 (2004) 5263.
[11] U. Kreibig, M. Vollmer, 1995. *Optical Properties of Metal Clusters*. Springer Verlag, New York.